

ADVANCED THOUGHTS ON THE INFILTRATION OF CERAMIC POROUS PLUGS BY LIQUID STEEL

L. O. Z. Falsetti*, D. N. F. Mucbe and V. C. Pandolfelli

Graduate Program in Materials Science and Engineering (PPGCEM), Materials Microstructure Engineering Group (GEMM), FIRE Associate Laboratory, Materials Engineering Department (DEMa), Federal University of São Carlos (UFSCar)

ABSTRACT

The control of non-metallic inclusion content during the secondary metallurgy is a key feature to ensure the quality of the steel. In a typical process, these particles are captured by bubbles generated by a porous plug located at the bottom of the ladle, whose structure consists of open pores that allow gas injection into the molten bath. On the other hand, liquid steel may penetrate through this porous structure during the non-bubbling period, solidifying as the ladle cools down. To remove this infiltrated thickness, an oxygen lance (at approximately 2000°C) heats the surface of the porous plug, in a cleaning procedure pointed out as the leading wear mechanism in such refractory. A classical approach to understand the infiltration of a liquid on a porous structure is based on the Washburn's equation and defines the start condition to liquid penetration. By applying the same Washburn's fundamentals to our study, a criterion to avoid liquid steel infiltration into the plug is determined. Herein, the influence of the pore diameter, the material composition and the gas counter-pressure on steel penetration is analysed. Based on these results, a feasible solution is proposed as a countermeasure to prevent the infiltration of porous plugs.

INTRODUCTION

Purging plugs are ceramic devices placed at the bottom of metallurgical ladles to provide the injection of inert gases, and consequently the generation of bubbles in the molten metal. The bubbling process aims at chemical and thermal

homogenization of the liquid metal, as well as the capture of inclusions. Thus, the selection of the purging plug among the commercially available models is directly related to its purpose, as their permeable structure comprises either slits or pores, such as the slot or porous plugs, respectively. Additionally, a combination of both structures led to the development of a hybrid plug with slits to provide high gas fluxes for the molten metal homogenisation and a porous insert aiming at generating smaller bubbles to capture inclusions¹. Regarding the production of clean steels, this study focuses on the porous structure, prevailing on hybrid plugs.

The metallurgical ladle holds various refractory linings and devices, and although the purging plug represents just one kind of those, its short lifespan can dictate the periodicity of the small-scale repairs^{2,3}. Therefore, a straightforward solution to extend the time among ladle maintenances is to reduce the plug wearing mechanisms such as chemical corrosion, abrasion and thermal spalling. However, Ouchi (2001)⁴ states that the cycle of metal infiltration and cleaning is the key source of damage, limiting the life span of a ceramic plug (see Fig. 1a-b).

As the injection of gas is carried out intermittently, the infiltration of liquid metal through the open porosity of the plug takes place at the non-bubbling period, resulting in serious damage to its structure². The infiltrated layer is partially withdrawn during the subsequent gas injection, and the clogged pores are cleared after the liquid steel is transferred to the tundish, as

This UNITECR 2022 paper is an open access article under the terms of the [Creative Commons Attribution License, CC-BY 4.0, which permits](https://creativecommons.org/licenses/by/4.0/) use, distribution, and reproduction in any medium, provided the original work is properly cited.

represented in Fig. 2. This cleaning process relies on heating the surface of the porous plugs with an oxygen lance under temperatures above 2100°C, leading to the melting of the infiltrated metal ⁵. In parallel, a gas flux applied from the bottom of the plug helps to expel the remaining molten steel.

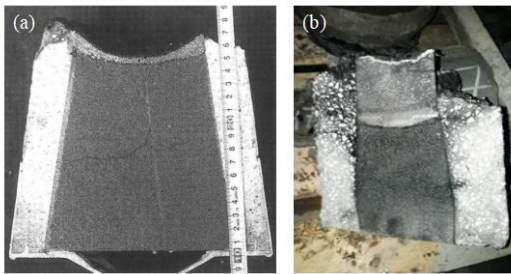


Fig. 1: Cut section of (a) a porous plug after use and before oxygen lance cleaning and (b) a hybrid plug, courtesy of RHI-Magnesita.

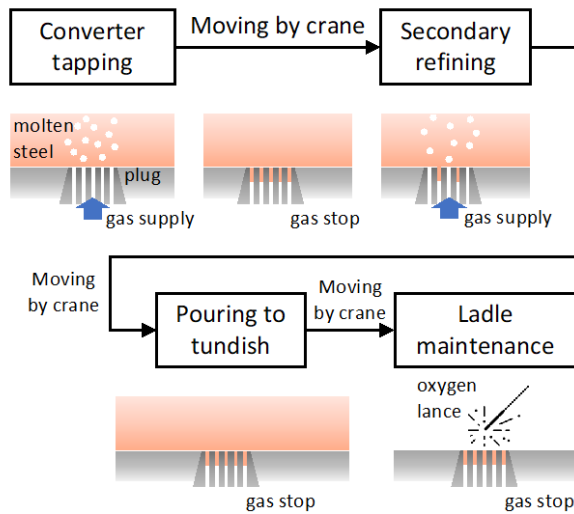


Fig. 2: Schematic representation of the infiltration and cleaning cycle in porous plugs. Adapted from ².

Understanding this process is not novel and dates back to the classical Washburn equation ⁶. Kaptay et al. ⁷ investigated different structures to predict the depth of penetration as a

function of the external pressure applied, concluding that a periodical porous structure could describe the experimental data for liquid metal infiltration in porous structures. To some extent, these concepts have been applied to porous plugs to analyse the effect of the pore diameter at the start and propagation of infiltration through the open porosity ⁸.

Additionally, the literature presents some experiments regarding the infiltration of purging plugs and, although some were carried out with slot plugs, their interpretations can also be applied to porous structures. Clasen et al. ⁹ studied the influence of liquid steel temperature, slit width and pressure difference on the infiltration of slot plugs, obtaining statistically equivalent depths in the range of 83 and 88mm for different combinations of these features. Thus, the work highlights that the infiltration depth is limited by the solidification of the liquid steel at the cold area of the plug (below 1514°C). Huang et al. ¹⁰ carried out a similar experiment which analysed the penetration of liquid slag in ceramic slits under a constant temperature profile. As there was no cold region along the slit, the infiltration depth changed due to the slit width and the liquid temperature. Therefore, limiting the infiltration depth to regions above the solidus temperature of the steel could allow one to flush out the liquid before it solidifies inside the porous structure of the ceramic plug.

The driving force to start and propagate the infiltration is the pressure acting at the liquid-gas interface of each pore. Thus, Eq. (1) describes the total pressure (P_{Σ}), which is comprised by the liquid capillarity (P_C), liquid column (P_G) and the external pressure difference (ΔP_o) ⁷.

$$P_{\Sigma} = P_C + P_G + \Delta P_o \quad (1)$$

As Eq. (1) is commonly associated to the mercury porosimetry test, some of these terms

must be modified when the application of purging plugs at the bottom of steel ladles is considered. Therefore, the pressure due to liquid capillarity in Eq. (2) can be stated as a function of the liquid-gas interfacial tension (σ_{lg}), the contact angle (θ) and the diameter of the pore (D). The pressure due to the gravity in Eq. (3) corresponds to the ferrostatic one (P_{Fe}), which depends on the liquid column height (H) and its density (ρ_l), and on the gravitational acceleration (g). ΔP_o in Eq. (4) is given by the difference between the atmospheric pressure (P_{atm}) and the absolute gas counter-pressure, or merely the relative gas counter-pressure (P_{gas}). Based on Eqs. (2)-(4), it can be concluded that P_G always favour the liquid penetration, whereas P_C and ΔP_o act in the opposite direction when $\theta > 90^\circ$ and $P_{gas} < 0$, respectively.

$$P_C = 4\sigma_{lg} \cos \theta / D \quad (2)$$

$$P_G = P_{Fe} = \rho_l g H \quad (3)$$

$$\Delta P_o = P_{atm} - P_{gas,abs} = -P_{gas} \quad (4)$$

Therefore, this works aims to evaluate the infiltration of the porous plug based on a fundamental perspective, by reviewing the current knowledge in the literature to describe the importance of each parameter when starting the penetration. Based on these results and industrial practice, improvements for the ceramic plug design and bubbling system setup are discussed.

MATERIALS AND METHODS

According to Kaptay et al. ⁷, $P_\Sigma \geq 0$ defines a criterion to start the infiltration, as represented in Fig. 3a. Thus, the opposite condition is considered to avoid the penetration of metal into the porous plug, and Eq. (5) is obtained by expanding the total pressure terms as in Eq. (1). By substituting equations (2)-(4) in equation (5) and rearranging them, Eq. (6) can be

obtained which defines the maximum pore diameter (D) to avoid the infiltration of liquid steel.

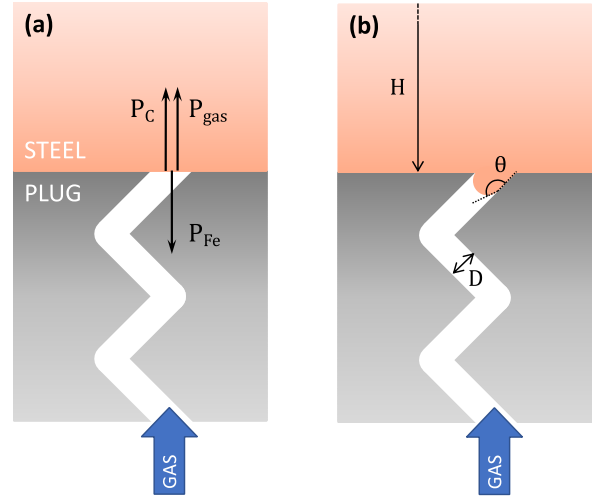


Fig. 3: Schematic representation of the (a) pressure terms and (b) parameters involved in the infiltration process, for $\theta > 90^\circ$.

$$P_C + P_G + \Delta P_o < 0 \quad (5)$$

$$D < \frac{-4\sigma_{lg} \cos \theta}{\rho_l g H - P_{gas}} \quad (6)$$

Eq. (6) point out the criteria to start the liquid penetration in each pore. Thus, the influence of the following parameters will be analysed:

- D_{max} : maximum pore diameter to avoid the start of liquid penetration;
- θ : contact angle defined by the plug material, as the liquid and gas phases are previously determined;
- D_{min} : minimum diameter along the capillary;
- P_{gas} : gas counter-pressure applied to the plug.

To obtain results that are close to the state-of-the-art practices in steelmaking industries, the hybrid plug (RHI-Magnesita) will be considered as

working system. Its chemical composition comprises mainly Al_2O_3 ¹, with a contact angle of 125° among the refractory, liquid iron and argon gas¹¹. The typical porous microstructure of these inserts presents an open porosity of about 27 vol.% on average¹² and a pore diameter of about $50\mu\text{m}$. Table I summarises the values for liquid iron used in this work, considering that the surface tension for liquid steel does not change significantly for carbon contents in the range of 0 to 0.1 at.%.¹³ Table II shows the physical properties of liquid steel and argon gas¹⁴. A ladle height of 3.5m will be considered for the calculations, corresponding to a ferrostatic pressure of 240kPa.

Table I: Contact angle among refractory, liquid iron and argon gas at 1600°C ¹¹.

Refractory	Al_2O_3	MgO	SiO_2
Contact angle (θ)	125°	130°	130°

Table II: Physical properties related to liquid steel and argon gas¹⁴.

Property	σ_{lg}	ρ_l
Value	1.82 N m^{-1}	7020 kg m^{-3}

RESULTS AND DISCUSSION

Plug structure

Based on Eq (6) and the system of study, one can calculate the maximum pore diameter (D_{max}) to avoid the start of liquid penetration depending on the contact angle (θ) among the solid, liquid and gas phases. To do this, the diameter of the pores in contact with liquid steel should be limited to $17\mu\text{m}$, which under argon flow will generate bubbles of 1.4mm , as represented in Fig. 4¹⁵. This bubble diameter is within the range to withdraw SiO_2 (1 to 5mm) and Al_2O_3 (0.5 to 2mm) inclusions¹⁶⁻¹⁸. On the other hand, such narrow pores would be virtually unfeasible

for the target application as the structure permeability could be significantly reduced.

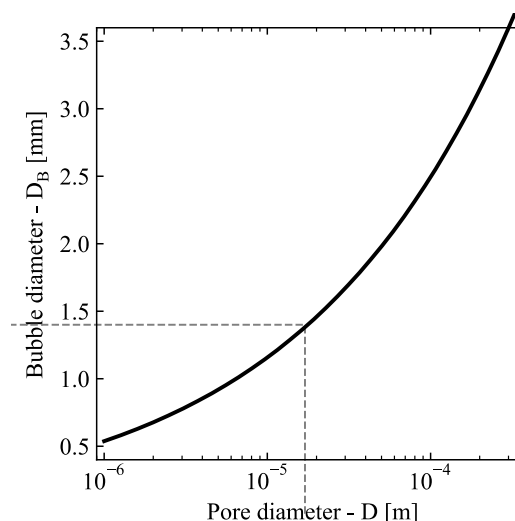


Fig. 4: Diameter of the generated bubble (D_B) as a function of the pore diameter (D).

Nevertheless, a second approach to avoid the infiltration for ceramics containing larger pores could be the increase of the θ angle. Fig. 5 shows the results for contact angles ranging from 90° to 180° , for a 3.5m high steel column with no counter-pressure gas applied. As the composition of the steel is defined by the process and the inert gas is restricted to Ar, a change in the contact angle could be attained by tuning the ceramic purging plug composition. However, as presented in Table I, the contact angle would increase from 125° for an Al_2O_3 plug to 130° for a MgO or SiO_2 ones, corresponding to a maximum pore diameter of $19\mu\text{m}$ for the latter. Besides, the contact angle among the gas atmosphere, the liquid metal and the ceramic refractory is defined by the equilibrium of the interfacial tensions, which are strongly influenced by the temperature, the oxygen partial pressure and the presence of other impurities¹⁹. Even assuming a non-wetting plug ($\theta \approx 180^\circ$), the maximum pore diameter would still be limited to

30 μ m for a 3.5m high liquid steel column. Therefore, the modification of the contact angle based on the plug material is also not a feasible alternative towards infiltration mitigation.

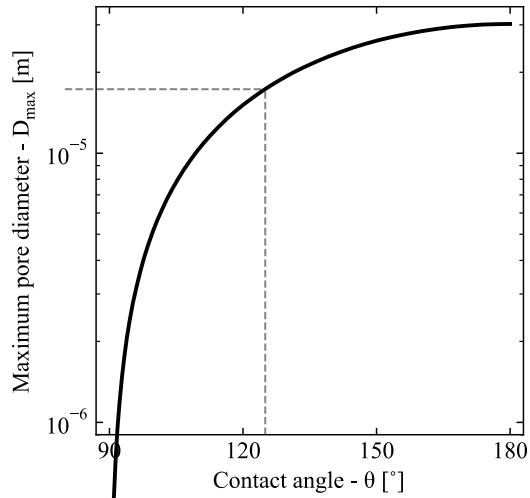


Fig. 5: Maximum pore diameter as a function of contact angle to inhibit metal infiltration, considering a steel column of 3.5m and no gas counter-pressure.

Even though the plug material on its own is not sufficient to avoid the infiltration of liquid steel, it is still important to look for chemical compositions with high contact angles, resulting in a capillary pressure that works inhibiting the liquid penetration. To properly select the plug material, other properties should also be considered, like the ones related to the thermal shock and corrosion aspects^{20,21}. However, the control of infiltration narrows the possibilities to compositions poorly wetted by liquid steel. In this sense, this discussion is in tune with the current commercial plugs, which are majorly composed of Al_2O_3 and MgO ^{1,12}.

It is also worth mentioning that slags typically have a low contact angle with ceramic refractories, for example, a MgO plug in contact with a $CaO-SiO_2-Al_2O_3$ (40/40/20) slag at 1400°C defines a θ value below 32°¹³. For $\theta <$

90°, the capillary force acts in favour of slag penetration into porous structures, and the infiltration occurs irrespectively of the liquid column height above the plug. Besides that, the high temperature of the steel ladle can lead to chemical reactions between the slag and plug so that the contact between these phases must be avoided.

Another point to be taken into account is that porous structures are not comprised by capillaries with a constant diameter, indicating that the minimum diameter along the capillary (D_{min}) can be located below the surface in contact with liquid steel, as represented in Fig. 6a. D_{min} could, in theory, refrain the propagation of molten metal infiltration to a lower depth in the ceramic plug. Although this approach seems to be reasonable at first glance, the interconnection among these capillaries in the porous structure makes it unviable, as liquid would still penetrate via parallel paths. This effect was experimentally assessed by Yamada et al.⁸, where the porous structures with a narrower pore diameter distribution presented a homogeneous infiltration of liquid steel (Fig. 6b), whereas a wider distribution exhibited clogged pores due to parallel infiltration through the largest ones, as represented in Fig. 6c.

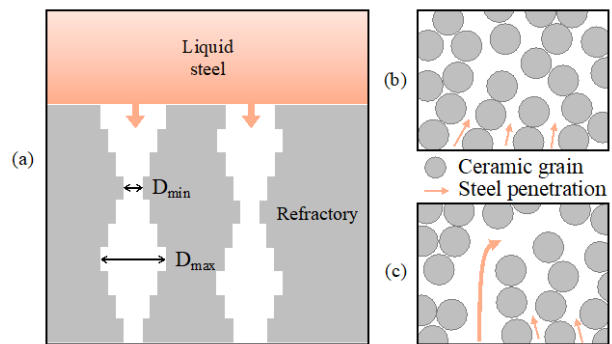


Fig. 6: Schematic representation of (a) pore diameter changes along the porous structure, and the influence of (b) a narrow and (c) a wide pore

diameter distribution on the steel penetration. Adapted from ^{8,22}.

Gas counter-pressure

A likely solution to avoid the initiation of molten steel infiltration in the ceramic porous structure consists of applying a gas counter-pressure, whose end value should be high enough to overcome the ferrostatic pressure. Eq. (6) can be rearranged to estimate the pressure needed to avoid the infiltration of liquid steel in a given structure, by isolating the P_{gas} term, which results in Eq. (7).

$$P_{\text{gas}} > \rho_l g H + 4 \sigma_{lg} \cos \theta / D \quad (7)$$

Fig. 7a shows the minimum gas counter-pressure to avoid infiltration initiation for liquid columns up to 4.5m and different values of pore diameter. As an example, a P_{gas} of at least 160kPa (1.58atm) should be applied to an alumina porous plug considering a 3.5m high liquid column and a pore diameter of 50 μm . It is worth noting that this pressure would not induce bubbling as this value is in equilibrium with the ferrostatic pressure (see yellow dotted line in Fig. 7a-b). Nevertheless, for the same conditions, keeping a counter-pressure above 250kPa could avoid the infiltration and provide the required bubbling.

Fig. 7b presents the minimum gas counter-pressure that must be applied to avoid the plug infiltration based on its contact angle and pore diameter. For a contact angle above 90°, a 250kPa gas pressure is higher than the ferrostatic pressure applied by the liquid steel column, therefore the plug would be bubbling at this pressure and the liquid penetration would not happen for the whole pore diameter range analysed. If this pressure was dropped to values below P_{Fe} (240kPa), the infiltration would start at the largest pores of the structure. On the other hand, the smallest pores will be infiltrated firstly for contact angles below 90°. This effect rises

from the wetting of the structure as the capillary pressure can act in favour or against infiltration depending on θ , and P_C magnitude increases with the reduction of the pore diameter (see Eq. (2)). For instance, SiC which presents a contact angle of 37° with liquid iron would not be a good material choice for the ceramic plug core regarding the control of infiltration ²³.

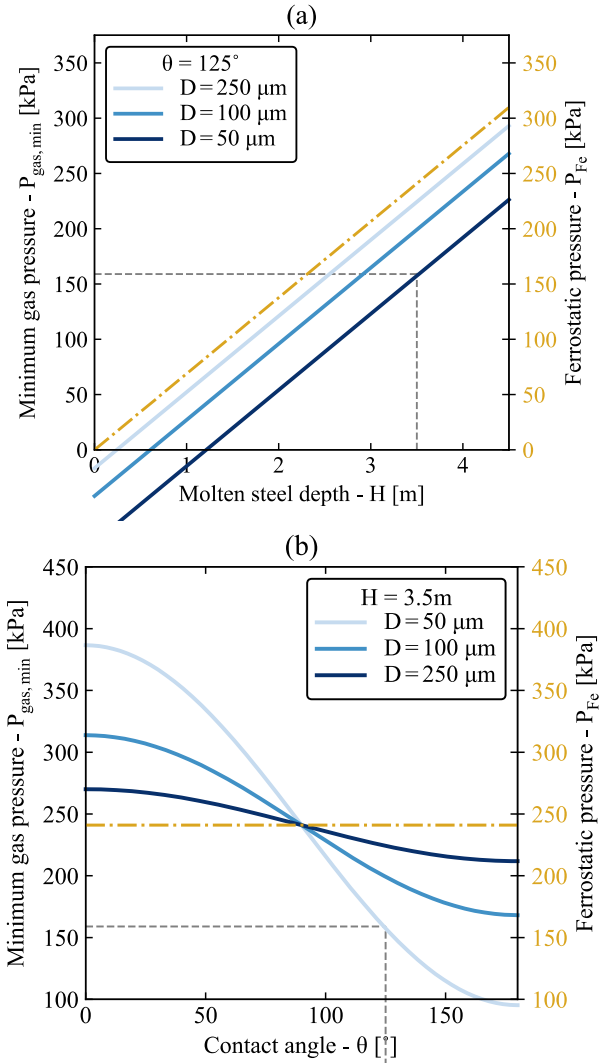


Fig. 7: Minimum gas counter-pressure as a function of (a) the liquid steel height and (b) the contact angle, for different values of pore

diameter and the corresponding ferrostatic pressure.

CONCLUSION

This work focused on evaluating liquid steel infiltration in porous structured plugs, based on the parameters that can control it. The effect of the plug composition (contact angle), pore diameter and applied gas pressure on the initiation of infiltration was investigated. The obtained results assessed experimental findings from the literature and industrial practices on ceramic plugs, analysing the contribution of each parameter and the feasibility of the likely countermeasures.

Results indicated that plug compositions with higher contact angles are more suitable to reduce the structure wearing, as the capillary pressure acts in opposition to the infiltration of liquid steel. The current commercial plugs are mainly comprised of Al_2O_3 , presenting a θ equal to 125° when in contact with molten steel, which defines a maximum pore diameter of $17\mu\text{m}$ to avoid infiltration. However, besides the thermal shock and corrosion aspects, the change to other materials such as MgO and SiO_2 would not result in considerable benefits as the maximum pore diameter would be limited to $19\mu\text{m}$.

The application of a gas counter-pressure on the alumina porous plug seemed to be a great tool to control the infiltration into the structure, as a pressure of 160kPa is sufficient to avoid the penetration into pores of $50\mu\text{m}$ or smaller. The results, discussions and most of the text of this article were based on the following publication: L.O.Z. Falsetti, D.N. Ferreira Muche, V.C. Pandolfelli, *Ceramics International* 47 26350–26356 (2021). Therefore, for further details about its content, please consult the original paper.

ACKNOWLEDGEMENTS

This study was financed in part by the Coordenação de Aperfeiçoamento de Pessoal de

Nível Superior - Brasil (CAPES) - Finance Code 001 - process 88887.639824/2021-00, and by the Conselho Nacional de Desenvolvimento Científico e Tecnológico - Brasil (CNPq) - process 130515/2019-1. The authors are also thankful to RHI-Magnesita and FIRE (Federation for International Refractory Research and Education) for supporting this research.

REFERENCES

1. RHI-Magnesita. Gas purging systems for steel casting and treatment ladles. <https://www.rhimagnesita.com/brochure/gas-purging-systems-for-steel-casting-and-treatment-ladles/> (2019).
2. Iio, Y., Tsukigase, H., Ito, S. & Satoh, M. Improvement of the refractory lining life of steel ladle. in *UNITECR Proceedings* 759–762 (2019).
3. Tan, F., He, Z., Jin, S., Li, Y. & Li, B. Study on failure and refining effect of purging plugs with different slits. *Refract. WorldForum* 13, 54–58 (2021).
4. Ouchi, T. Wear and countermeasures of porous plugs for ladle. *J. Tech. Assoc. Refract. Japan* 21, 270–275 (2001).
5. Ogata, K., Kago, T. & Matsumura, K. Evaluation method of porous plug durability simulating actual condition. in *UNITECR Proceedings* 768–771 (2019).
6. Washburn, E. W. The dynamics of capillary flow. *Phys. Rev.* 17, 273–283 (1921).
7. Kaptay, G., Matsushita, T., Mukai, K. & Ohuchi, T. On different modifications of the capillary model of penetration of inert liquid metals into porous refractories and their connection to the pore size distribution of the refractories. *Metall. Mater. Trans. B* 35, 471–486 (2004).
8. Yamada, K., Oishi, T., Matsumoto, S. & Ouchi, T. Three-dimensional analysis of

- porous plug structure using X-ray CT. in *UNITECR Proceedings* 581–584 (2019).
9. Clasen, S., Sax, A. & Quirnbach, P. Analysis of molten steel infiltration into analysis slits of purging plugs. *Refract. Worldforum* **12**, 72–76 (2020).
 10. Huang, A., Fu, L., Gu, H. & Wu, B. Towards slag-resistant, anti-clogging and chrome-free castable for gas purging. *Ceram. Int.* **42**, 18674–18680 (2016).
 11. Zhao, L. Interfacial phenomena and chemical reactions during interactions of iron and graphite/oxide substrates for refractory applications. (University of New South Wales, 2003).
 12. Trummer, B., Fellner, W., Viertauer, A., Kneis, L. & Hackl, G. A water modelling comparison of hybrid plug, slot plug and porous plug designs. *RHI Bull.* 35–38 (2016).
 13. Nakashima, K. & Mori, K. Interfacial properties of liquid iron alloys and liquid slags relating to iron- and steel-making processes. *ISIJ Int.* **32**, 11–18 (1992).
 14. Liu, H., Qi, Z. & Xu, M. Numerical simulation of fluid flow and interfacial behavior in three-phase argon-stirred ladles with one plug and dual plugs. *Steel Res. Int.* **82**, 440–458 (2011).
 15. Mori, K. Kinetics of fundamental reactions pertinent to steelmaking process. *Trans. Iron Steel Inst. Japan* **28**, 246–261 (1988).
 16. Zhang, L. & Taniguchi, S. Fundamentals of inclusion removal from liquid steel by bubble flotation. *Int. Mater. Rev.* **45**, 59–82 (2000).
 17. Wang, L., Lee, H. G. & Hayes, P. Prediction of the optimum bubble size for inclusion removal from molten steel by flotation. *ISIJ Int.* **36**, 7–16 (1996).
 18. Falsetti, L. O. Z., Ferreira Muche, D. N., Santos Junior, T. dos & Pandolfelli, V. C. Thermodynamics of smart bubbles: The role of interfacial energies in porous ceramic production and non-metallic inclusion removal. *Ceram. Int.* **47**, 14216–14225 (2021).
 19. Ni, P., Goto, H., Nakamoto, M. & Tanaka, T. Neural network modelling on contact angles of liquid metals and oxide ceramics. *ISIJ Int.* **60**, 1586–1595 (2020).
 20. Long, B., Andreas, B. & Xu, G. Thermodynamic evaluation and properties of refractory materials for steel ladle purging plugs in the system Al₂O₃-MgO-CaO. *Ceram. Int.* **42**, 11930–11940 (2016).
 21. Long, B., Xu, G., Buhr, A., Jin, S. & Harmuth, H. Fracture behaviour and microstructure of refractory materials for steel ladle purging plugs in the system Al₂O₃-MgO-CaO. *Ceram. Int.* **43**, 9679–9685 (2017).
 22. Cheng, Z. & Zhu, M. Theoretical analysis and experiment of liquid metal penetration into slot plug applied for refining ladles. *Metall. Mater. Trans. B* **45**, 1695–1705 (2014).
 23. Nogi, K. & Ogino, K. Wettability of SiC by liquid pure metals. *Trans. Japan Inst. Met.* **29**, 742–747 (1988).